

Correlated ab-initio calculations for ground-state properties of II-VI semiconductors

Martin Albrecht and Beate Paulus

Max-Planck-Institut für Physik komplexer Systeme, Bayreuther Straße 40, D-01187 Dresden, Germany

Hermann Stoll

Institut für Theoretische Chemie, Universität Stuttgart, D-70550 Stuttgart, Germany

Correlated *ab-initio* ground-state calculations, using relativistic energy-consistent pseudopotentials, are performed for six II-VI semiconductors. Valence (ns, np) correlations are evaluated using the coupled cluster approach with single and double excitations. An incremental scheme is applied based on correlation contributions of localized bond orbitals and of pairs and triples of such bonds. In view of the high polarity of the bonds in II-VI compounds, we examine both, ionic and covalent embedding schemes for the calculation of individual bond increments. Also, a partitioning of the correlation energy according to local ionic increments is tested. Core-valence ($nsp, (n-1)d$) correlation effects are taken into account via a core-polarization potential. Combining the results at the correlated level with corresponding Hartree-Fock data we recover about 94% of the experimental cohesive energies; lattice constants are accurate to $\sim 1\%$; bulk moduli are on average 10% too large compared with experiment.

I. INTRODUCTION

Ab initio calculations for solids are mostly performed nowadays formally within a one-particle picture using density-functional theory (DFT), i.e. describing the non-local exchange together with many-particle correlation effects within the local-density approximation (LDA)¹ or within more sophisticated generalized-gradient approximations (GGA)². As an alternative, it is possible at the one-particle level to calculate the non-local exchange of a solid exactly, using a periodic Hartree-Fock (HF) scheme³.

However, for a proper microscopic treatment of electron correlations it is necessary to go beyond the one-particle framework and to deal with many-body wave functions. In the case of finite systems, accurate quantum-chemical methods, of the configuration interaction (CI) or coupled-cluster (CC) type, have been developed for the determination of many-body wave functions and the corresponding correlation energies. In the case of solids, the latter methods are not directly applicable, but it is often possible, to a very good approximation, to cast the correlation energy of the infinite system into a rapidly converging expansion in terms of increments from localized orbital subsystems⁴. Due to the local character of the correlation hole these increments may be determined for finite fragments of the solid and, as a consequence, the correlation energy of the solid becomes accessible to a quantum-chemical treatment.

The method of local increments has been applied to elementary⁵ and III-V semiconductors⁶, with an expansion in terms of correlation contributions related to localized bond orbitals and to pairs and triples of such bonds. On the other hand, the same method has also successfully been used for ionic compounds such as MgO, CaO, and NiO⁷; there, the local increments refer to groups of atomic orbitals which can be assigned to given anionic or cationic centers. In an attempt to bridge the gap between covalent and ionic solids we now investigate the use of incremental schemes for correlation effects in II-VI semiconductors.

In Section II, we present the results of Hartree-Fock self-consistent field (SCF) calculations for the solids just mentioned. The inclusion of correlations is discussed in Section III; we first focus on the various correlation effects which have to be considered, and then elaborate on embedding procedures and the computational details of the method. Results follow in Section IV. Finally, pertinent conclusions are given in Section V.

II. HARTREE-FOCK CALCULATIONS

A starting point for treating many-body correlation effects in solids are reliable Hartree-Fock self-consistent field results for the infinite system. We performed HF ground-state calculations for six II-VI semiconductors, i.e., ZnS, ZnSe and ZnTe and the corresponding Cd compounds in the zinc-blende structure, using the program package CRYSTAL92⁸.

The large number of electrons and the relativistic effects occurring in these materials can efficiently be handled by means of pseudopotentials. For the group VI elements we use the scalar-relativistic energy-consistent pseudopotentials of Bergner et al., together with the corresponding $(4s5p)/[3s3p]$ atomic valence basis sets⁹. For their application in the CRYSTAL calculations the basis sets have to be modified, however: very diffuse exponents which are necessary to properly describe the tails of the free-atom wavefunctions cause numerical problems in CRYSTAL. In the solid the basis functions of neighbouring atoms take over their role due to close-packing. Therefore we leave out the most diffuse p exponent and use a reduced atomic $(4s4p)/[3s3p]$ basis set supplemented by a d polarization function, which has been optimized for the Zn-compounds in the solid ($d_S=0.45$, $d_{Se}=0.35$, $d_{Te}=0.25$).

TABLE II. Crystal-optimized basis sets for 20-valence-electron and 2-valence-electron pseudopotentials of Zn and Cd. In parentheses, we list the additional exponents and contraction coefficients of the atomic basis used in the calculations of the free atoms as well as in the cluster calculations.

	<i>s</i> -exp.	coeff.	<i>p</i> -exp.	coeff.	<i>d</i> -exp.	coeff.
Zn	27.785554	0.1074375	92.652341	0.0024709	61.208798	0.0220562
20-ve	17.520914	-0.1821469	19.771450	-0.0781854	19.141955	0.1188778
	10.282040	-0.3099337	4.465187	0.4036449	6.873575	0.3064757
	2.755438	1	1.908780	0.525450	2.517245	0.4305467
	1.169907	1	0.758772	1	0.858306	0.363375
	0.187	1	0.10	1	0.25	1
	0.11	1				
Zn	1.572755	0.313862	1.025	1 (-0.076200)	0.235	1
2-ve	1.198905	-0.541801	0.26	1 (0.269338)		
	0.20 (0.148856)	1	0.13627	1		
	0.10 (0.051016)	1	(0.0415)			
Cd	10.497284	0.4871518	5.130033	-0.5067959	8.890067	-0.0138837
20-ve	6.998189	-1.0501142	3.420022	0.6070007	2.964186	0.2810514
	4.665459	0.0728619	1.282189	0.6495556	1.231907	0.4924337
	1.465187	1	0.543303	0.2159152	0.465127	0.3622932
	0.654782	1	0.169429	1	0.15	1
	0.355802	1	0.08	1		
	0.08	1				
Cd	1.298843	0.240843	0.581900	1 (-0.192137)	0.203	1
2-ve	0.865895	-0.534798	0.337511	1 (0.227533)		
	0.202302	1 (0.232332)	0.095653	1		
	0.090463	1	(0.033746)			
	(0.037232)	1				

For the group IIb elements Zn and Cd we use two different sets of pseudopotentials: first 20-valence-electron pseudopotentials, where the outer-core $(n-1)d$ shell and the corresponding $(n-1)s, p$ shells are explicitly treated together with the ns, p valence electrons^{10,11}. Again, optimized $(8s7p6d)/[6s5p3d]$ basis sets are available (which we use for the calculation of the free atoms), but a re-optimization is needed for the solid. Leaving out the most diffuse s and p exponents of the atomic basis sets (for Cd the outer d exponent, too), we determined, for each angular momentum independently, the smallest exponent which still leads to a stable solution in the CRYSTAL calculation. Starting with these (fixed) outer exponents we reoptimized the inner ones yielding $(7s6p6d$ or $7s6p5d)/[5s4p2d]$ basis sets (see Table II).

Furthermore, we use large-core 2-valence electron pseudopotentials for Zn¹²(see Table I) and Cd¹³ (which will also be used at the correlated level, cf. Sect. 3). For Zn, a $(4s2p)$ basis set is available in the literature¹². Since in the materials which we are concerned with (polarized) bonds between sp^3 -hybrids are formed, we added two inner p functions optimized in a Hartree-Fock calculation for the first excited $s^1p^1\ ^3P$ atomic state. The outermost p exponent is subsequently left out in the CRYSTAL calculation; in addition, the two most diffuse s functions are reoptimized for the solid, and a d polarization function is added, yielding a $(4s3p1d)/[3s3p1d]$ basis set (see Table II). For the Cd pseudopotential¹³ no basis set exists in the literature. We therefore first optimized a $(5s4p)$ basis

TABLE I. The Zn 2-valence-electron pseudopotential is represented in the semilocal form $V_{PP}(r_i) = -\frac{Q}{r_i} + \sum_{l=0}^{l_{\max}} \sum_k A_{lk} \exp(-\alpha_{lk} r_i^2) P_l$, where P_l is the projection operator onto the Hilbert subspace of angular symmetry l . The exponents α_{lk} and the coefficients A_{lk} are listed below.

l	α_{lk}	A_{lk}
s	1.4988020	18.31672
	0.7490050	-3.405011
p	1.5327700	11.46430
	0.7870910	-1.327391
d	0.7502760	1.583946
	0.3747920	0.333476
f	0.4666990	-0.398428

in a Hartree-Fock calculation for the first excited $s^1p^1\ ^3P$ atomic state. For the solid, the outer s and p exponents were neglected, and a d exponent was optimized yielding a $(4s3p1d)/[3s3p1d]$ basis set (see Table II).

Using the small-core pseudopotentials for Zn and Cd with their corresponding basis sets we determined SCF ground state energies of the solids. To estimate the numerical accuracy of the CRYSTAL results (for a detailed discussion see Ref.[8]), we performed various test calculations concerning the computational parameters for ZnS, the system with the smallest lattice constant. The convergence with respect to the ‘Coulomb overlap’ parameter is very good yielding an error of less than 10^{-5} Hartree.

The ‘Coulomb penetration’ parameter which controls the Coulomb series is more critical. We could not reach any monotonous convergence, the deviation between the two ‘best’ parameters pointing to an uncertainty of the order of 10^{-4} Hartree. Concerning the exchange series a similar behaviour is found. The convergence with respect to the ‘exchange overlap’ is very good (error less than 10^{-5} Hartree), whereas the parameters affecting the ‘exchange penetration’ are very critical. Due to the quite diffuse basis functions we had to use, we could only reach an accuracy of the order of 10^{-4} Hartree. Thus, for ZnS we end up with an error bar of $\pm 3 \cdot 10^{-4}$ Hartree. The finite k -point sampling for the reciprocal-space integration causes errors of less than 10^{-5} Hartree, which can be neglected in comparison with the error due to the truncation of the Coulomb and exchange series.

For evaluating cohesive energies, we subtracted the ground-state energies of the free atoms obtained with the corresponding atom-optimized basis sets; the quantum-chemical *ab-initio* program system MOLPRO94¹⁴ was used in these latter calculations. The results for SCF cohesive energies at the experimental lattice constants¹⁵ applying the small-core pseudopotentials for Zn and Cd are listed in the first column of Table VI. A comparison is made to experimental cohesive energies (last column in Table VI) which are corrected by phonon zero-point energies $\frac{9}{8}k_B\Theta_D$ (derived from the Debye model¹⁶) as well as by atomic spin-orbit splittings¹⁷. It is seen that binding energies at the HF level are between 60% and 70% of the experimental values leaving room for significant correlation contributions.

For determining lattice constants and bulk moduli, we performed a 4th order polynomial fit to the SCF ground-state energies evaluated within a range of -2% to $+6\%$ of the experimental lattice constant, in half-percent steps. The deviations between calculated and fitted points are of about $\pm 1 \cdot 10^{-4}$ Hartree. The lattice constants (listed in Table VII) obtained from the minimum of the polynomial fit are too large, by up to 4.5%, as compared to experiment. When applying different kinds of fits, to all calculated points as well as to those surrounding the minimum only, the lattice constants change by at most $\pm 0.01\text{\AA}$ ($\sim 0.2\%$). Thus, we conclude that correlation corrections are important for the lattice constants, too. The bulk modulus of cubic structures can be determined according to

$$B = \left(\frac{4}{9a} \frac{\partial^2}{\partial a^2} - \frac{8}{9a^2} \frac{\partial}{\partial a} \right) E_{\text{total}}(a), \quad (1)$$

where a is the lattice constant. The second term is only zero if we calculate the bulk modulus at the minimum of the potential curve. The first and especially the second derivative of the potential curve are much more affected by the errors of the total energy than the position of the minimum of the curve. Taking into account all points in the range of -2% to $+6\%$ of the experimental lattice constant, the total-energy error can be estimated to

lead to an uncertainty of about $\pm 2\%$ for the bulk modulus; with only seven points around the minimum this error bar would increase to up to $\pm 15\%$. We therefore performed a 4th order polynomial fit to all points when determining $\frac{\partial E}{\partial a}$ and $\frac{\partial^2 E}{\partial a^2}$. Additionally, we tested polynomial fits of other degrees: we find that 3rd, 4th or 5th order fits differ by about $\pm 3\%$ only, whereas a quadratic fit would yield bulk moduli smaller by up to 20%. We calculated the bulk moduli at the Hartree-Fock lattice constant and at the experimental one. The bulk moduli at the Hartree-Fock lattice constant are too small by up to $\sim 30\%$, compared with the experiment, mainly due to the drastic overestimation of the lattice constants. The Hartree-Fock bulk moduli calculated at the experimental lattice constant, on the other hand, are by up to 30% higher than the experimental ones. Again, this points to the necessity of correlation corrections.

In order to check the influence of an explicit treatment of the d shells for Zn and Cd, we determined the cohesive energies and lattice constants of ZnS and CdS using the large-core pseudopotentials and corresponding basis sets as described above. For ZnS we reach 72%, for CdS 73% of the experimental cohesive energy, while the lattice constants are overestimated by 1% only. However, the better agreement with experiment is due to a spurious compensation of the (still missing) correlation effects; with the metal d shells incorporated into the pseudopotential, the closed-shell repulsion of these shells on the valence electrons of the neighbouring atoms becomes too weak, cf. Ref. 18 for a thorough discussion in a molecular context. This does not mean, on the other hand, that large-core pseudopotentials should not be applied at all for Zn and Cd. Since closed-shell repulsion is mainly a Hartree-Fock effect, correlation contributions are expected to come out quite similar as with the small-core pseudopotentials. This expectation is fully borne out by test calculations to be discussed in the following section.

III. MANY-BODY CORRECTIONS

A. Treatment of correlation effects

There are two important contributions of electron correlation which we have to consider in our calculations. The largest piece of the correlation energy is due to the correlated motion of the valence electrons. We account for it by applying the method of local increments to be explained in the second part of this subsection. Intershell outer-core–valence correlations have little influence on the cohesive energy but are important for the calculation of the lattice constants and the bulk moduli. They are efficiently simulated via a core-polarization potential¹⁹.

1. Core-polarization potential

The implicit description of core electrons by means of pseudopotentials or the explicit freezing of closed core shells at the Hartree-Fock level implies a neglect of static and dynamic core polarization. The former effect being due to static electric fields is zero, for symmetry reasons, in isotropic solids of the type considered here. The latter part, however, is non-zero and is related to core-valence correlations. Especially with closed outer-core d -shells the influence of dynamic core polarization on bond lengths is known to be significant¹⁹, from molecular calculations. We simulate this effect by means of a core polarization potential (CPP), which describes the charge-induced dipole interaction between valence electrons and cores:

$$V_{\text{CPP}} = - \sum_{\lambda} \frac{1}{2} \alpha_{\lambda} \vec{f}_{\lambda}^2; \quad (2)$$

Here α_{λ} is the dipole polarizability of core λ , and \vec{f}_{λ} is the field at site λ generated by valence electrons and surrounding cores:

$$\vec{f}_{\lambda} = \sum_i^{N_V} \frac{\vec{r}_{\lambda i}}{r_{\lambda i}^3} \left(1 - e^{-\delta_{\lambda} r_{\lambda i}^2}\right) - \sum_{\mu (\neq \lambda)} \frac{\vec{r}_{\lambda \mu}}{r_{\lambda \mu}^3} \left(1 - e^{-\delta_{\lambda} r_{\lambda \mu}^2}\right); \quad (3)$$

$r_{\lambda i}$ is the distance between valence electron i and core λ , N_V is the number of valence electrons, and $r_{\lambda \mu}$ the distance between two cores. The cut-off parameter δ_{λ} is necessary in order to remove the singularity of the dipole interaction at $r_{\lambda i} = 0$. We took the parameters α_{λ} and δ_{λ} from Ref. 13, where the CPP was adjusted in atomic calculations to the spectra of single-valence-electron ions. Adding V_{CPP} (eq. 1) to the valence Hamiltonian in large-core pseudopotential SCF calculations corresponds to correlated calculations with simultaneous (single) excitations from both core and valence-shell orbitals. Using the CPP in calculations, where the valence electrons are correlated, the additional coupling between core-valence and valence correlations is accounted for.

2. Method of increments

We determine (valence) correlation effects in infinite systems using an expansion in terms of local increments. Here we only want to sketch the basic ideas and some important formulae. A formal derivation and more details can be found in Ref. [5]. The method relies on localized orbital groups (labeled I, J) generated in a SCF reference calculation using a suitable localization criterion (such as that of Foster and Boys²⁰). The orbital groups may comprise single localized bond orbitals, in the case of covalently bonded solids, or all of the (modified) atomic

orbitals which can be assigned to an ion in the case of ionic solids. One-body correlation-energy increments ϵ_I are obtained by correlating each group of the localized orbitals separately while keeping the other ones inactive. In the present work we use the coupled-cluster approach with single and double substitutions (CCSD). This yields a first approximation to the correlation energy

$$E_{\text{corr}}^{(1)} = \sum_I \epsilon_I, \quad (4)$$

which corresponds to the correlation energy of independent ions or independent bonds.

In the next step we include correlations of pairs of orbital groups. Only the non-additive part $\Delta\epsilon_{IJ}$ of the two-body correlation energy ϵ_{IJ} is needed.

$$\Delta\epsilon_{IJ} = \epsilon_{IJ} - (\epsilon_I + \epsilon_J). \quad (5)$$

Higher order increments are defined analogously. For the three-body increment, for example, one has

$$\Delta\epsilon_{IJK} = \epsilon_{IJK} - (\epsilon_I + \epsilon_J + \epsilon_K) - (\Delta\epsilon_{IJ} + \Delta\epsilon_{JK} + \Delta\epsilon_{IK}). \quad (6)$$

The correlation energy of the solid is finally obtained by adding up all the increments with appropriate weight factors:

$$E_{\text{corr}}^{\text{solid}} = \sum_I \epsilon_I + \frac{1}{2!} \sum_{\substack{IJ \\ I \neq J}} \Delta\epsilon_{IJ} + \frac{1}{3!} \sum_{\substack{IJK \\ I \neq J \neq K}} \Delta\epsilon_{IJK} + \dots \quad (7)$$

It is obvious that by calculating higher and higher increments the exact correlation energy within CCSD is determined. However, the procedure described above is only useful if the incremental expansion is well convergent, i.e., if increments up to, say, three-body increments are sufficient, and if increments rapidly decrease with increasing distance between localized orbital groups. These conditions were shown to be well met in the case of covalently bonded solids^{5,6}, with an expansion in terms of localized bond orbitals, and for ionic compounds like alkali halides²¹ or various oxides⁷, using orbital groups of ions as basic entities. When applying the method of increments to II-VI semiconductors we have to check which orbital partitioning is more suitable and efficient, from a physical as well as a computational point of view. Since this question also touches that of cluster embedding, to be dealt with in the next subsection, we shall postpone its discussion to Sec.III C.

B. Embedding procedure

Due to the local character of dynamical correlations, the increments defined in the previous section should

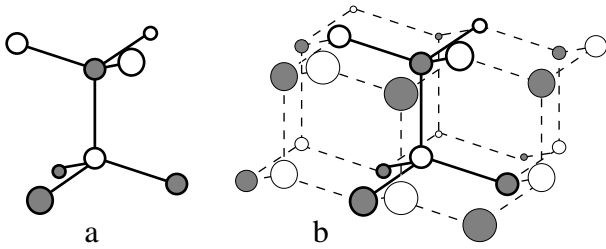


FIG. 1. Figure a shows the X_4Y_4 cluster, where the white circles indicate the group IIb elements, the shaded circles the group VI elements; the hydrogen atoms are not drawn. Figure b shows the $X_{13}Y_{13}$ cluster, where the white/shaded circles connected by solid lines indicate the group IIb/VI elements which are treated in the full basis set; the hydrogen atoms are not drawn.

be fairly local entities. We use this property to calculate these increments in finite fragments of the solid. Thereby, an appropriate embedding procedure simulating the influence of the infinite system surrounding the chosen cluster is of crucial importance.

For non-polar or only slightly polar semiconductors we use a saturation of the dangling bonds with hydrogen atoms. As an example, a $X_4Y_4H_{18}$ cluster is shown in Fig. 1a. All the bond angles are chosen to be tetrahedral. The X—H and Y—H distances, respectively, are optimized in CCSD calculations for a XYH_6 cluster yielding $d_{ZnH}=1.6643\text{\AA}$, $d_{CdH}=1.7913\text{\AA}$, $d_{SH}=1.3468\text{\AA}$, $d_{SeH}=1.4658\text{\AA}$ and $d_{TeH}=1.6510\text{\AA}$. We performed test calculations for the II-VI semiconductors using the $X_4Y_4H_{18}$ cluster with the experimental XY distances of the solid. What we find is a net charge transfer of about 0.6 electrons (according to a Mulliken population analysis), from the hydrogen atoms bonded to group VI elements to the hydrogen neighbours of the group IIb atoms. This is mainly due to the electro-negativity of the group VI elements being larger than that of hydrogen. In order to avoid this charge transfer which generates an unphysical charge distribution for the inner bonds, we tested a more sophisticated approach to hydrogen saturation.

The X_4Y_4 cluster is surrounded by an additional shell of X and Y atoms at the sites of the bulk solid, whose dangling bonds in turn are saturated with hydrogens (see Fig. 1b). This yields a $X_{13}Y_{13}H_{30}$ cluster which is still amenable to an *ab-initio* quantum-chemical treatment, provided the additional X, Y atoms are treated with reduced accuracy (minimal $(1s1p)$ basis set). Now, the charge transfer is much smaller than in the $X_4Y_4H_{18}$ cluster, but a slight charge transfer of about 0.2 electrons still persists, from the upper plane where the group IIb elements are located, to the lower plane built up from the group VI elements. This could only be avoided if the embedding in minimal-basis-set atoms were symmetrical with respect to the inner X_4Y_4 fragment. This would result in a $X_{22}Y_{22}H_{42}$ cluster, which is too large for our calculations.

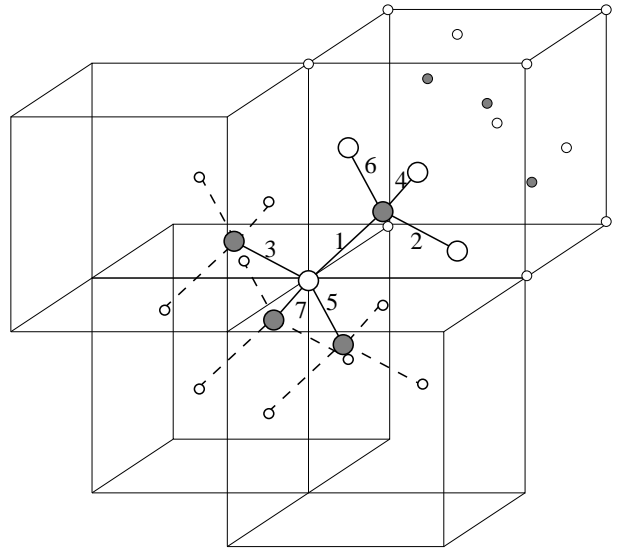


FIG. 2. Figure 2 shows the point charge embedding; in the center the X_4Y_4 cluster treated with the full basis set (big circles connected by solid lines); the smaller circles connected by dashed lines indicate the group IIb elements described with minimal basis. In the upper right cube we show representatives for the $4 \times 4 \times 4$ point-charge embedding (unconnected circles, white circle +2, shaded circle -2).

Another possibility is the embedding with point charges. Here, one can proceed to a very large surrounding, virtually without increasing the computation time for the inner fragment. The X_4Y_4 cluster is surrounded by point charges, with the group IIb and group VI atoms simulated by point charges +2 and -2, respectively (see Fig. 2). We extended the point-charge region to $4 \times 4 \times 4$ unit cells. The point charges on the outer planes have the values ± 1 , on the edges $\pm \frac{1}{2}$ and on the corners $\pm \frac{1}{4}$. (An analogous procedure works well for ionic compounds with NaCl-structure [7,21].)

For the II-VI semiconductors there is a problem with the point-charge embedding: the electrons are too strongly localized at the outer group VI atoms. In the infinite solid, there is a charge transfer, of about one electron (according to Mulliken's population analysis), from each of the group VI ions to the group IIb neighbours. In order to properly allow for this charge transfer in our cluster model, we replace the point charges by large-core pseudopotentials, together with $(4s4p)/[1s1p]$ basis sets, for the group IIb neighbours of the central X_4Y_4 unit. (The p function is necessary to generate the directional bonds.) The modified point charge embedding for the X_4Y_4 cluster is shown in Fig.2.

We have tested all three embedding schemes just mentioned in calculations for Zn compounds. We calculated the one-bond increment for the central bond of the X_4Y_4 unit, all two-bond increments up to second nearest neighbours, and neighbouring three-bond increments; the correlation energies obtained are listed in Table III. Although ZnS has the largest difference in

TABLE III. Test calculations for the valence correlation energy (in Hartree per unit cell) using different embedding schemes, cf. text. The calculations are performed with basis A without the core-polarization potential; third-nearest-neighbour bond contributions are neglected.

cluster model	ZnS	ZnSe	ZnTe
$X_4Y_4H_{18}$	-0.1893	-0.1758	-0.1700
$X_{13}Y_{13}H_{30}$	-0.1847	-0.1650	-0.1489
X_4Y_4 + point charges	-0.1813	-0.1637	-0.1420

electro-negativity, the three embedding schemes yield very similar results. For ZnTe, the simple saturation with hydrogen fails, whereas the embedding in atoms with minimal basis and the embedding in point charges provide similar results (error less than 5%). The correlation contributions obtained with the point-charge embedding are in all cases smaller than those of the covalent cluster models, probably due to the more severe restriction of the external space. Nevertheless, we favour the point-charge embedding because of the higher computational efficiency.

We also tested the influence of the core-polarization potential on the lattice constant, for the three cluster models of ZnSe, but found no difference between the simple saturation with hydrogen atoms and the point-charge embedding. This shows that core-valence correlation is an even more local entity than valence correlations.

C. Computational details

Calculating correlation-energy increments will be done in two steps. First core-valence correlations are simulated in SCF calculations with core-polarization potentials included for the two inner atoms of the X_4Y_4 cluster. Due to the local character of core polarization (cf. Ref. [6b]), the incremental energy contributions from the X and Y atoms are additive and directly transferable to the solid. The second step, i.e. the determination of valence correlations and post-SCF core-polarization contributions is more difficult. We first have to decide which partitioning of the localized orbitals is appropriate for the II-VI semiconductors. For the elementary and III-V semiconductors it is natural to build up the method of increments in terms of localized bonds, pairs and triples of such bonds; an accuracy of 1% of the correlation energy can be reached by carrying the correlation-energy expansion up to third nearest neighbour two-bond increments and nearest-neighbour three-bond increments. It seems reasonable to check whether such a scheme still works for the II-VI systems. Bond increments up to second-nearest neighbours are accessible from the X_4Y_4 cluster shown in Fig. 2. For deriving increments involving third-nearest neighbours, we use the clusters shown in Fig. 3. As an example, we list the increments obtained for ZnTe, together with the appropriate weight factors, in Table IV.

TABLE IV. Correlation-energy increments for ZnTe (in Hartree), determined at the CCSD level using basis set A. For the numbering of the clusters and bonds involved, see Figs. 2 and 3.

	cluster	Increment	Weight factor
incremental expansion in terms of bonds			
ϵ_I	$X_4Y_4/1$	-0.0119037	4
$\Delta\epsilon_{IJ}$	$X_4Y_4/1,2$	-0.0082766	6
	$X_4Y_4/1,3$	-0.0017476	6
	$X_4Y_4/2,3$	-0.0003937	12
	$X_4Y_4/2,5$	-0.0003238	24
	Fig.3a/1,4	-0.0001562	6
	Fig.3a/2,5	-0.0000446	6
	Fig.3b/2,5	-0.0001166	24
	Fig.3b/3,6	-0.0000388	24
	Fig.3b/4,7	-0.0000984	12
	Fig.3b/1,4	-0.0000531	12
	Fig.3c/1,4	-0.0001490	12
$\Delta\epsilon_{IJK}$	$X_4Y_4/1,2,4$	+0.007866	4
	$X_4Y_4/1,3,5$	+0.0001350	4
	$X_4Y_4/1,2,3$	-0.0000030	12
	$X_4Y_4/1,2,5$	+0.0000308	24
E_{corr}		-0.124408	
incremental expansion in terms of ions			
ϵ_I	X_7Y_2	-0.097605	1
$\Delta\epsilon_{IJ}$	X_7Y_2	-0.004927	6
E_{corr}		-0.127170	

The other possibility of orbital partitioning is the ionic approach⁷. Here, the localized orbitals are exclusively assigned to one of the electro-negative group VI atoms. The group defining a one-body increment comprises the four sp^3 -type bond orbitals connected to a given anion; accordingly, the nearest-neighbour two-body increments are built up from the orbital groups assigned to two neighbouring group VI atoms. The calculations are performed for a X_7Y_2 cluster (see Fig. 3). (A further extension is computationally not feasible, at present: inclusion of group VI atoms beyond nearest neighbours would result in very large clusters, higher-order increments would involve correlation of 24 or more electrons. Thus, we cannot fully check the convergence of this approach.) The one-body and nearest-neighbour two-body increment for ZnTe are listed in the second part of Table IV. Although the two approaches are not equivalent, neither with respect to the number of orbitals simultaneously correlated nor with respect to the truncation criteria for the distance of correlated orbitals, the correlation energies differ by 2% only. This shows that we can bridge the gap between incremental expansions appropriate for covalent and ionic solids in an unequivocal way.

In the calculations including valence correlations we used large-core pseudopotentials for Zn and Cd combined with CPPs. In order to check the reliability of the large-core pseudopotentials for determining correlation contributions, we performed test calculations for ZnS, ZnTe and CdS. We calculated the one-bond increment in an

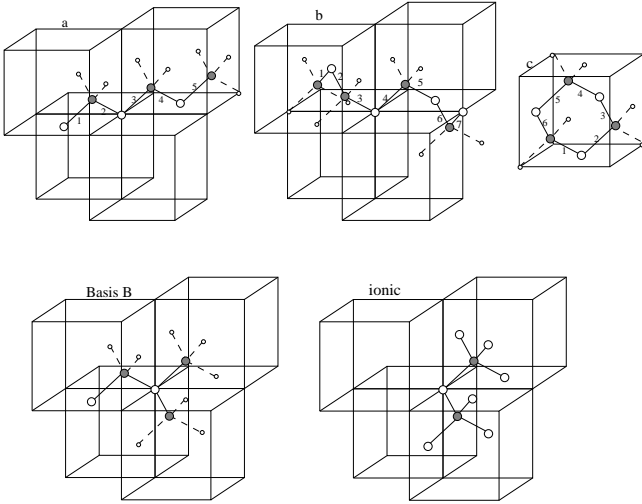


FIG. 3. In the first line, we show the clusters used for deriving third-nearest-neighbour increments; the second line refers to calculations employing basis B and the X_7Y_2 cluster used in the ionic approach, respectively. The notation and point-charge embedding is the same as in Figure 2.

XY_4 cluster using alternatively the 20-valence-electron and the 2-valence-electron pseudopotentials for $X = \text{Zn}, \text{Cd}$. The absolute values of the increments obtained differ by 5 mHartree, but the physically important differential correlation contributions to the cohesive energy differ by 1.5 mHartree at most, which is less than 1% of the cohesive energy. Therefore, for our purposes, the large-core pseudopotentials can be considered as sufficiently accurate.

Two different basis sets are used in our calculations. Basis A is of valence-double-zeta quality. For the group VI elements we choose the $(4s5p)/[3s3p]$ valence basis set by Bergner et al.⁹, cf. also Sect. II. For Zn, we start from the $(4s2p)$ valence basis of Ref. 12, add the same inner p functions as in the Hartree-Fock calculation and end up (after contraction) with a $[3s3p]$ basis set (cf. Table 2, numbers in parentheses). For Cd, the atom-optimized primitive $(5s4p)$ basis set of Sect. 2 is contracted to $[3s3p]$, too (cf. Table 2, numbers in parentheses). Furthermore, for each of the elements, we supply one d polarization function whose exponent is optimized in CCSD calculations for the free atom (see Table V, first column).

An enlarged basis B is generated by uncontracting the sp valence basis sets to $[4s4p]$ and replacing the single d function by a $2d1f$ polarization set. The exponents of the latter are energy-optimized in CCSD calculations for the free atoms (see Table V). This basis is only applied to the five largest increments which can be calculated in a X_2Y_3 cluster (see Fig.3).

For hydrogen saturation, we use Dunning's double-zeta basis²² (without p polarization function), or, in the case of the $X_{13}Y_{13}$ clusters, its fully contracted (minimal basis set) version.

TABLE V. Polarization functions used in the CCSD calculations.

	basis A, 1d	basis B, 2d1f		
Zn	0.235	0.157	0.330	0.312
Cd	0.203	0.163	0.240	0.268
S	0.479	0.269	0.819	0.557
Se	0.343	0.197	0.462	0.478
Te	0.221	0.177	0.281	0.360

IV. RESULTS AND DISCUSSION

We applied the method of increments, as formulated in terms of localized bond orbitals, for calculating the core-valence (cv) and valence (vv) correlations of six II-VI compounds. As the first ground state property we calculated the cohesive energy at the experimental lattice constant (see Table VI). At the Hartree-Fock level, where we use the small-core pseudopotentials for Zn and Cd, we reach only between 60% and 70% of the experimental value. Core-valence correlations have virtually no effect on the cohesive energy; for the Zn-compounds they increase it by about 1%, for the Cd-compounds they yield a reduction of about the same percentage. Valence correlations, on the other hand, have a significant influence on the cohesive energy. With basis set A, the cohesive energy is increased by about 20%, with basis B even by about 30%. This corresponds to about 60% and 85%, respectively, of the correlation contribution to the cohesive energy. On the average, we recover 97% of the experimental cohesive energy for the Zn-compounds. For the Cd-compounds, the agreement is less perfect (about 91%); it may be possible that an extended basis for Cd, including g functions, yields further improvement. Errors due to the truncation of the incremental expansion can be estimated to about $\pm 3\%$. According to Harrison²³, the experimental error of the cohesive energy, due to measuring the heat of formation and the heat of atomization at different temperatures, is $\sim 1\%$. A comparison of our results with density-functional ones from literature is only possible for ZnSe, to the best of our knowledge; the LDA value reported in Ref. [23] is 0.212 Hartree which corresponds to an overestimation of 8%. The percentage of the cohesive energy reached in our present calculations is comparable to that for the elementary and III-V semiconductors^{5,6} as well as to that for the ionic systems^{7,21}, showing that our approach works well also for intermediate systems.

As in the case of cohesive energies, Hartree-Fock lattice constants are far from the experimental values, with deviations of up to 4.5%. In this case, however, the core-valence effects are decisive; they reduce the lattice constants by about 3% (see Table VII), whereas valence correlations have only a small influence. The latter fact is related to the opposite trends caused by inter- and intra-atomic correlations; as a result, valence correlations can lead to a net increase *or* decrease of the lattice con-

TABLE VI. Cohesive energies per unit cell (in Hartree), at different theoretical levels (cf. text); the Hartree-Fock values are obtained with small-core pseudopotentials for Zn and Cd, whereas the correlation calculations are performed with large-core pseudopotentials. Deviations from experimental values²³ (in percent) are given in parentheses.

	HF		HF+cv		HF+cv+vv basis A		HF+cv+vv basis B		exp
ZnS	0.159	(68%)	0.160	(68%)	0.204	(87%)	0.224	(95%)	0.236
ZnSe	0.135	(69%)	0.136	(70%)	0.183	(94%)	0.196	(100%)	0.196
ZnTe	0.115	(64%)	0.117	(65%)	0.155	(86%)	0.174	(97%)	0.180
CdS	0.129	(62%)	0.127	(61%)	0.168	(80%)	0.187	(89%)	0.211
CdSe	0.110		0.109		0.151		0.166		
CdTe	0.099	(60%)	0.099	(60%)	0.132	(80%)	0.153	(93%)	0.164

TABLE VII. Lattice constants (in Å) at different theoretical levels (cf. text); the Hartree-Fock values are obtained with small-core pseudopotentials for Zn and Cd, whereas the correlation calculations are performed with large-core pseudopotentials. Deviations from experimental values measured at room temperature are given in parentheses.¹⁵

	HF		HF+cv		HF+cv+vv basis A		LDA		exp
ZnS	5.5908	(+3.3%)	5.4512	(+0.8%)	5.4355	(+0.5%)	5.42 ^b	(+0.2%)	5.4100
ZnSe	5.8849	(+3.8%)	5.7386	(+1.3%)	5.7290	(+1.1%)	5.7839 ^a	(+2.0%)	5.6676
ZnTe	6.3752	(+4.4%)	6.1982	(+1.5%)	6.1827	(+1.3%)	6.1279 ^a	(+0.4%)	6.1037
CdS	6.0465	(+3.9%)	5.8730	(+0.9%)	5.8853	(+1.2%)	5.85 ^b	(+0.6%)	5.8180
CdSe	6.3254	(+4.5%)	6.1315	(+1.3%)	6.1583	(+1.7%)	6.07 ^b	(+0.3%)	6.0520
CdTe	6.7746	(+4.4%)	6.5434	(+0.9%)	6.5640	(+1.2%)	6.40 ^b	(-1.3%)	6.4860 ¹

¹ calculated from the wurtzite structure

^a Reference[25]

^b Reference [26]

TABLE VIII. Bulk moduli (in Mbar) at different theoretical levels (cf. text); the Hartree-Fock values are obtained with small-core pseudopotentials for Zn and Cd, whereas the correlation calculations are performed with large-core pseudopotentials. Deviations from (averages of) experimental values¹⁵ are given in parentheses.

	HF, min		HF, exp		HF+cv		HF+cv+vv		LDA		exp
ZnS	0.744	(-3%)	0.924	(+21%)	0.799	(+4%)	0.770	(+1%)	0.81 ^b	(+5%)	0.748...0.784
ZnSe	0.634	(0%)	0.885	(+39%)	0.766	(+20%)	0.738	(+16%)	0.605 ^a	(-5%)	0.624...0.647
ZnTe	0.434	(-22%)	0.734	(+32%)	0.629	(+13%)	0.604	(+9%)	0.501 ^a	(-3%)	0.50...0.612
CdS	0.593	(-9%)	0.911	(+40%)	0.792	(+22%)	0.795	(+22%)	0.70 ^b	(+14%)	0.615...0.69
CdSe	0.406	(-29%)	0.727	(+34%)	0.615	(+7%)	0.616	(+7%)	0.66 ^b	(+20%)	0.55...0.60
CdTe	0.337	(-29%)	0.604	(+27%)	0.498	(+5%)	0.498	(+5%)	0.52 ^b	(+15%)	0.425...0.528

^a Reference[25]

^b Reference [26]

stant. For the lighter compounds, basis A is sufficient to describe the shortening of the bonds caused by intra-atomic correlations, whereas for the heavier compounds basis A increases the lattice constant and a decrease is observed only with the enlarged basis B (for example in CdTe: $a_{\text{basisA}}^{cv+vv}=6.5640\text{\AA} \geq a^{cv}$ and $a_{\text{basisB}}^{cv+vv}=5.5437\text{\AA} \leq a^{cv}$, whereas for ZnS $a_{\text{basisA}}^{cv+vv}=5.4360\text{\AA} \leq a^{cv}$ and $a_{\text{basisB}}^{cv+vv}=5.4275\text{\AA} \leq a^{cv}$). A comparison with LDA results shows that we reach about the same level of accuracy as Vogel et al.²⁶, who treated correlation effects with a self-interaction-corrected (SIC) pseudopotential.

The bulk moduli (see Table VIII) calculated from the first and second derivative of the potential curve at the experimental lattice constant are too large at the Hartree-Fock level. Due to the uncertainties of the Hartree-Fock ground-state energy values (cf. Sect. II), it is unreasonable to add the correlation energies to the Hartree-Fock ones and perform a fitting of the full potential curve: the influence of correlations on the bulk modulus would be partly suppressed by the 'noise' of the Hartree-Fock values. Therefore we separately fitted the core-valence and the valence correlation-energy contributions through a quadratic fit, calculated the first and second derivatives of these curves at the experimental lattice constant, and added them to the corresponding Hartree-Fock derivatives. For the core-valence correlations, we determined the energy contributions in the whole Hartree-Fock region, with steps of 1% in the lattice constant. These differential energies have numerical errors of less than 10^{-5} Hartree, which yields negligible errors for the bulk moduli; the subsequent fitting introduces errors of about $\pm 2\%$. The core-valence correlations reduce the bulk moduli significantly, by about 20% on the average, mainly due to the instantaneous deformation of the cores in the field of the valence electrons. The influence of the valence correlations, which are calculated at five points around the experimental lattice constant, is much smaller. With basis A, they reduce the bulk moduli of the Zn-compounds by about 4%. For the Cd-compounds the reduction is below 1% with basis A; for CdTe, where we also applied basis B, there is an reduction of about 4%. Overall, the calculated bulk moduli are about 10% too large compared with mean experimental values. The error bars in our calculations can be roughly estimated to $\pm 7\%$, all in all; if we define experimental error bars through the spread of the various experimental values, they are of the same order of magnitude as our theoretical ones. LDA calculations reach the same level of accuracy. The advantage of our approach is that we can discuss the influence of various electron-correlation effects on the lattice constant and the bulk modulus at a microscopic level.

V. CONCLUSION

We have determined ground-state properties (cohesive energies, lattice constants, bulk moduli) of six II-VI semiconductors, at various theoretical levels. The Hartree-Fock results have been obtained using the solid-state program CRYSTAL92, explicitly treating the outer-core d shell of Zn and Cd with small-core pseudopotentials and crystal-optimized basis sets. For the cohesive energies, we recover between 60% and 70% of the experimental values. The lattice constants are overestimated by up to 4.5% and the bulk moduli, evaluated at the experimental lattice constants, are too large. Accounting for core-valence correlations by means of core-polarization potentials has only a slight influence on cohesive energies but yields a large reduction of the lattice constants and the bulk moduli. Correlations of the valence electrons are determined with the help of an incremental expansion in terms of localized bonds, and pairs and triples of such bonds; individual increments are evaluated at the coupled-cluster (CCSD) level, for fragments of the solid in a point-charge embedding. Including valence correlations, we reach 85% of the correlation contributions to the cohesive energies, or $\sim 95\%$ of the total experimental values. Valence correlations reduce the lattice constants only slightly, leading to final values within 1% of the experimental data; there is also moderate decrease of the bulk moduli.

The present calculations show that a reliable microscopic description of electron-correlation effects in II-VI semiconductors can be obtained in terms of local excitations, and that a unified treatment (with uniform accuracy) is possible this way for a variety of ionic as well as covalently bonded solids.

-
- ¹ R. O. Jones and O. Gunnarsson, Rev. Mod. Phys. **61**, 689 (1989).
 - ² J. P. Perdew, in *Density Functional Theory*, edited by E. K. U. Gross and R. M. Dreizler (Plenum Press, New York, 1995), p. 51.
 - ³ C. Pisani, R. Dovesi, and C. Roetti, in *Hartree-Fock Ab initio Treatment of Crystalline Systems*, edited by G. Berthier et al., Lecture Notes in Chemistry, Vol. **48** (Springer, Berlin, 1988).
 - ⁴ H. Stoll, Phys. Rev. B **46**, 6700 (1992).
 - ⁵ B. Paulus, P. Fulde, and H. Stoll, Phys. Rev. B **51**, 10572 (1995).
 - ⁶ B. Paulus, P. Fulde, and H. Stoll, Phys. Rev. B **54**, 2556 (1996); S. Kalvoda, B. Paulus, P. Fulde, and H. Stoll, Phys. Rev. B **55**, 4027 (1997); B. Paulus, F.-J. Shi, and H. Stoll, J. Phys. Cond. Matter **9**, 2745 (1997);
 - ⁷ K. Doll, M. Dolg, P. Fulde and H. Stoll, Phys. Rev. B **52**, 4842 (1995); K. Doll, M. Dolg, and H. Stoll, Phys. Rev. B

- 54**, 13529 (1996); K. Doll, M. Dolg, P. Fulde and H. Stoll, Phys. Rev. B **55**, 10282 (1997);
- ⁸ R. Dovesi, V. R. Saunders, and C. Roetti, *Computer Code Crystal 92*, Gruppo di Chimica Teorica, University of Torino and United Kingdom Science and Engineering Research Council Laboratory, Daresbury, 1992.
- ⁹ A. Bergner, M. Dolg, W. Küchle, H. Stoll and H. Preuss, Mol. Phys. **80**, 1431 (1993).
- ¹⁰ M. Dolg, U. Wedig, H. Stoll, and H. Preuss, J. Chem. Phys. **86**, 866 (1986).
- ¹¹ D. Andrae, U. Häussermann, M. Dolg, H. Stoll, and H. Preuss, Theor. Chim. Acta **77**, 123 (1990).
- ¹² M. Dolg and Fischer, unpublished results.
- ¹³ G. Igel-Mann, PhD thesis, University of Stuttgart (1987)
- ¹⁴ MOLPRO is a package of *ab initio* programs written by H.-J. Werner and P.J. Knowles, with contributions from J. Almlöf, R.D. Amos, A. Berning, C. Hampel, R. Lindh, W. Meyer, A. Nicklass, P. Palmieri, K.A. Peterson, R.M. Pitzer, H. Stoll, A.J. Stone, and P.R. Taylor; C. Hampel, K. Peterson and H.-J. Werner, Chem. Phys. Lett. **190**, 1 (1992); P.J. Knowles, C. Hampel and H.-J. Werner, J. Chem. Phys. **99**, 5219 (1993).
- ¹⁵ *Semiconductors: Physics of II-VI compounds*, ed. By K.-H. Hellwege, Landolt-Börnstein, New Series, Group III, vol. 17, pt. b, (Springer, Berlin, 1982).
- ¹⁶ B. Farid and R. Godby, Phys. Rev. B **43**, 14248 (1991).
- ¹⁷ C.E. Moore, Atomic Energy Levels, Circ. Nat. Bur. Stand. 467 (US Dept. of Commerce, Washington DC, 1958)
- ¹⁸ T. Leininger, A. Nicklass, H. Stoll, M. Dolg, and P. Schwedtfeger, J. Chem. Phys. **105**, 1052 (1996).
- ¹⁹ W. Müller, J. Flesch, and W. Meyer, J. Chem. Phys. **80**, 3297 (1984); P. Fuentealba, H. Preuss, H. Stoll and L. v. Szentpály, Chem. Phys. Lett. **89**, 418 (1982); A. Nicklass and H. Stoll, Mol. Phys. **86**, 317 (1995).
- ²⁰ J.M. Foster and S.F. Boys, Rev. Mod. Phys. **32**, 296 (1960).
- ²¹ K. Doll and H. Stoll, submitted to Phys. Rev. **B** (1997).
- ²² T. H. Dunning, J. Chem. Phys. **90**, 1007 (1989).
- ²³ W. A. Harrison, *Electronic structure and the properties of solids*, Dover Publications, Inc., New York (1989).
- ²⁴ A. Continenza, S. Massidda, and A. J. Freeman, Phys. Rev. B **38**, 12996 (1988).
- ²⁵ B. Freytag, and U. Rössler, J. Cryst. Growth **138**, 499 (1994).
- ²⁶ D. Vogel, P. Krüger, and J. Pollmann, Phys. Rev. B **54**, 5495 (1996).